Master's Thesis of Medical Science

Population pharmacokinetic analysis of two formulations of empagliflozin following a single oral dose in healthy adults

건강한 성인에서 empagliflozin 두 제제를 단회 투여 후 약동학 특성을 탐색하기 위한 집단 약동학 분석

August 2023

Graduate School of Department of Medicine
Seoul National University
Interdisciplinary Program of Clinical Pharmacology Major

Xu Jiang

Population pharmacokinetic analysis of two formulations of empagliflozin following a single oral dose in healthy adults

Submitting a master's thesis of Medical Science

April 2023

Graduate School of Department of Medicine
Seoul National University
Interdisciplinary Program of Clinical Pharmacology Major

Xu Jiang

Confirming the master's thesis written by
Xu Jiang
July 2023

Chair _____(Seal)
Vice Chair _____(Seal)
Examiner _____(Seal)

ABSTRACT

Population pharmacokinetic analysis of two formulations of empagliflozin following a single oral dose in healthy adults

Xu Jiang
Interdisciplinary Program of Clinical Pharmacology Major
Graduate School of Department of Medicine
Seoul National University

Background: Empagliflozin is a sodium-glucose cotransporter 2 (SGLT2) inhibitor that is commonly used for the treatment of type 2 diabetes mellitus (T2DM). As cocrystal formulation can improve the chemical properties of drugs, CKD-370 was newly developed as a cocrystal formulation of empagliflozin with solvate L-proline which has been confirmed the bioequivalence in South Korea. The aim of this study was to develop a population pharmacokinetic (pop-PK) model for two empagliflozin formulations in Korean healthy subjects and to explore the correlation between those two formulations and to investigate possible effects of various covariates on PK parameters of empagliflozin.

Methods: Total 864 plasma concentration data of 25 mg empagliflozin were obtained from 27 healthy adults and were used for the pop-PK analysis of empagliflozin. A pop-PK model was conducted by using a nonlinear mixed effects (NLME) approach (Monolix Suite 2021R1). Dataset included 13 potential covariates. Both inter-individual variability (IIV) and inter-occasion variability (IOV) were investigated. Final model was conducted both internal and external evaluation by goodness of fit (GOF) diagnostic plots, visual predictive checks (VPCs), prediction errors and bootstrapping.

Results: The pharmacokinetics (PK) of empagliflozin were adequately described with a 2-compartment model with 6 transit compartments with first-order absorption and elimination. The log-transformed body weight significantly influenced systemic clearance (CL) and the volume of distribution in peripheral compartment (V2) of empagliflozin. CKD-370 showed slower absorption than the empagliflozin. GOF plots, VPCs, prediction errors and bootstrapping of the final model suggested that the proposed model was adequate and robust with good precision also in the different dose strength.

Conclusion: The final population PK model for two empagliflozin formulations adequately described the observed plasma concentration of empagliflozin in healthy adults. This model is expected to understand the correlation of two empagliflozin

formulations and their PK characteristics. Furthermore, we first describe the establishment of a population PK model of empagliflozin in healthy Koreans that might be useful for customizing empagliflozin or exploring additional covariates in patients.

Keyword : Empagliflozin, Empagliflozin L-proline (CKD-370), population pharmacokinetic modeling

Student Number : 2021-29727

Table of Contents

ABSTRACT i

Table of Contents iv

List of Tables vi

List of Figures vii

List of Abbreviations x

Chapter 1. Introduction 1 3

1.1. Study Background 1 3

1.2. Purpose of Research 1 6

Chapter 2. Methods 1 7

2.1. Data and Study Population 1 7

2.2. Sample Collection and Analytical Methodology 1 8

2.3. Base Model Development 1 9

2.4. Covariate Analysis 2 1

2.5. Internal Evaluation of Final Model 2 2

2.6. External Evaluation of Final Model 2 3

Chapter 3. Results 25

3.1. Demographics and Datasets 25

3.2. Development of Base Model 27

3.3. Covariate Analysis 30

3.4. Internal Evaluation of Final Model 35

3.5. External Evaluation of Final Model 40

Bibliography 52

Abstract in Korean 58

List of Tables

Table 1. Demographic and biochemical information of the studied subjects (n = 27). 26

Table 2. Comparison of different pharmacokinetic models of empagliflozin. 28

Table 3. Estimates of the population pharmacokinetics parameter. 33

Table 4. Demographic and biochemical information of the subjects in the external evaluation dataset (n = 27). 41

Table 5. Summary of pharmacokinetic parameters of two empagliflozin formulations in plasma after single oral dose. .. 47

Table 6. Shrinkage of PK parameters. 49

List of Figures

Figure 1. Structural formula of empagliflozin L-proline(CKD-370). 15

Figure 2. The study design of comparative PK, phase I clinical trial. 17

Figure 3. Empagliflozin pop-PK model. 2-compartment transit model with first-order absorption and elimination best fitted observed empagliflozin plasma concentrations. 29

Figure 4. Goodness-of-fit plots of final population pharmacokinetic model for empagliflozin. (A) Population predicted concentrations (PRED) against observed plasma concentration; (B) Individual-predicted concentrations (IPRED) against observed plasma concentration; (C) Time against conditional weighted residuals; (D) PRED against conditional weighted residuals. Red dots mean the data are not censored. 37

Figure 5. Normalized prediction distribution error (NPDE) metrics for the population pharmacokinetic model of cefepime. Normal Q-Q plot for NPDE (A), distribution of NPDE (B), and NPDE versus time after first dose (C) and versus predicted concentrations (D). 38

Figure 6. Visual predictive check (500 simulations) of the final model

for empagliflozin. Observed concentrations were depicted by dots. Blue solid lines indicate 95th, 50th, and 5th percentiles of predicted concentrations. Black dash lines indicate the predicted mean. Blue shaded regions indicate 95% confidence intervals for predicted 5th and 95th percentiles. Pink shaded regions indicate 95% confidence intervals for the predicted 50th percentiles. Outliers are highlighted with red dots and areas. 39

Figure 7. Goodness-of-fit plots for external model evaluation. (A) Population-predicted concentrations (PRED) against observed plasma concentration; (B) Individual-predicted concentrations (IPRED) against observed plasma concentration; (C) Time against conditional weighted residuals; (D) PRED against conditional weighted residuals. Red dots mean the data are not censored. 42

Figure 8. NPDE for the validation set. a Q-Q plot. b Histogram of NPDE. Theoretical distribution represented as shaded bars. c NPDE versus time after dose (TAD). Prediction intervals represented as shaded areas. Observations plotted as circles and observation percentiles as solid lines. d NPDE versus PRED. 43

Figure 9. Visual predictive check (500 simulations) of the external model evaluation. Observed concentrations were depicted by dots. Blue solid lines indicate 95th, 50th, and 5th percentiles of

predicted concentrations. Black dash lines indicate the predicted mean. Blue shaded regions indicate 95% confidence intervals for predicted 5th and 95th percentiles. Pink shaded regions indicate 95% confidence intervals for the predicted 50th percentiles. Outliers are highlighted with red dots and areas. 44

Figure 10. Mean (SD) plasma concentration-time profile for single dose administration of two empagliflozin formulations in (A) linear scale and (B) log scale. 48

List of Abbreviations

ALP	Alkaline phosphatase
ALT	Alanine transaminase
AST	Aspartate aminotransferase
APE	Absolute prediction error
AUC	Area under the concentration-time curve
AUC_{last}	AUC from time zero to the last observation
AUC_{inf}	AUC from time zero to infinity
BIC	Bayesian information criterion
BLQ	Below the limit of quantification
BMI	Body mass index
C_{max}	Maximum plasma concentration
CI	Confidence interval
CL	Total apparent clearance
COSSAC	Conditional sampling use for stepwise approach based on correlation
CV	Coefficient of variation
CWRES	Conditional weighted residual errors
EDTA	K2-ethylenediaminetetraacetic
eGFR	Estimated glomerular filtration rate
FDC	Fixed dose combination

GOF	Goodness-of-fit
HbA1c	Glycated hemoglobin
IIV	Inter-individual variability
IOV	Inter-occasion variability
IPRED	Individual predictions
k_a	First order absorption rate constant
Ktr	Transit rate constant
LC	Loose combination
MDAPE	Median absolute prediction error
MDPE	Median prediction error
MPE	Mean prediction error
Mtt	Mean transit time
LC-MS/MS	Liquid chromatography with tandem mass spectrometry
LDH	Lactate dehydrogenase
NLME	Nonlinear mixed effects
NPDE	Normalized prediction distribution errors
OFV	Objective function value
PE	Prediction error
PK	Pharmacokinetics
Pop-PK	Population Pharmacokinetics

PRED	Population predictions
Q	Inter-compartmental clearance
RSE	Relative standard errors
SAEM	Stochastic Approximation Expectation Maximization
SD	Standard deviation
SGLT2	Sodium-glucose cotransporter 2
T2DM	Type 2 diabetes mellitus
$T_{1/2}$	Half-life
T_{max}	Time to reach maximum plasma concentration
V_1	The volume of distribution in central compartment
V_2	The volume of distribution in peripheral compartment
VPCs	Visual predictive checks

Chapter 1. Introduction

1.1. Study Background

Type 2 diabetes represents approximately 90% of global diabetes diagnoses with increasing prevalence worldwide [1]. It is characterized by hyperglycemia, insulin resistance, and relative impairment in insulin secretion [2]. Patients with T2DM are prone to macrovascular complications such as cardiovascular disease as well as microvascular complications that may affect the kidney, retina, and nervous system [3]. Therefore, blood sugar control is required to treat T2DM and to prevent complications. So far, several antidiabetic drugs with different mechanisms of action have been developed and approved for T2DM treatment, researchers are continually exploring new approaches to managing this complex disease.

Sodium-glucose cotransporter 2 (SGLT2) inhibitors, a class of hypoglycemic agent that works by inhibiting glucose reabsorption in the kidneys, resulting in increased glucose excretion in the urine and lower blood glucose levels was first developed in 2013 [4]. Empagliflozin (Jardiance®), a representative SGLT2 inhibitor, was first launched in 2014 under license from Boehringer Ingelheim International GmbH, Ingelheim, Germany [5]. Empagliflozin is a commonly used SGLT2 inhibitor that has been shown to be effective

in reducing blood glucose levels and improving cardiovascular outcomes in people with T2DM [6]. The pharmacokinetic (PK) studies of empagliflozin in healthy subjects were conducted in many countries [7–10], which showed rapid absorption after oral administration and a biphasic elimination [11].

Currently, because of the importance of the cocrystal form that can improve the performance of a dosage form [12], cocrystal technology is well known and widely used in the pharmaceutical industry to enhance the pharmaceutical product performance, such as mechanical properties, stability, solubility, permeability, dissolution rate of drugs to facilitate the development pharmaceutical formulation [5, 13–15]. Such as Suglat® (ipragliflozin L–proline), was firstly developed with solvate L–proline. Moreover, a novel dapagliflozin di–L–proline cocrystal–loaded tablet with low hygroscopicity and low water content was developed to solve the problems caused by the severe hygroscopic properties of dapagliflozin, such as inaccurate weighing, sticking in the compression process, and instability [16].

As co–crystallization of drugs with appropriate co–formers becoming a promising approach for enhancing oral absorption [14, 17, 18], empagliflozin L–proline, also was known as CKD–370 has been developed and approved in South Korea in 2021. CKD–370 is a newly developed co–crystalized formulation of empagliflozin with a solvate

of L-proline (Figure 1). It was proved that it can be broken down to empagliflozin in the digestive system and be absorbed in the form of empagliflozin (data on file). This new formulation has not yet been widely studied, and the bioequivalence study between CKD-370 and empagliflozin was conducted in 2019. Pharmacokinetics, safety, tolerability and bioequivalence of these two formulations were confirmed through the study. However, because of the formulation differences, more research is needed to fully understand the PK characteristics in absorption phase of CKD-370 compared to empagliflozin.

The population PK (pop-PK) models of empagliflozin in type 2 diabetes patients were developed in 2013 [19], however, up to now, no pop-PK studies of empagliflozin have been conducted in healthy subjects.

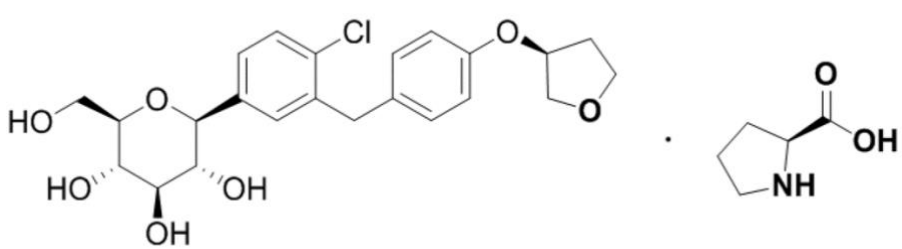

Figure 1. Structural formula of empagliflozin L-proline (CKD-370).

1.2. Purpose of Research

The aim of this study was to develop a pop-PK model of these two empagliflozin formulations in Korean healthy subjects and to explore both inter-individual variability (IIV) and inter-occasion variability (IOV) and their absorption differences between these two formulations, also to investigate the possible effects of various covariates on PK parameters of empagliflozin that can provide information for individualized medicine related to the study agent.

Chapter 2. Methods

2.1. Data and Study Population

Based on the PK data obtained from a comparative PK study [20], single administration of 25 mg empagliflozin and CKD-370 in 27 healthy Korean subjects, we developed a pop-PK model of empagliflozin. The comparative PK study was an open-label, randomized, two-period, two-sequence, crossover phase I study (NCT03849495). All subjects were divided into 2 groups with different treatment sequences (Figure 2). Subjects were administered empagliflozin followed by CKD-370 (sequence A) or CKD-370 followed by empagliflozin (sequence B). The washout period between each period was 7 days.

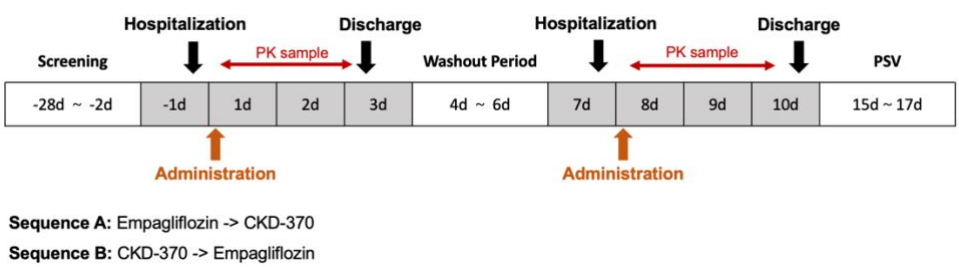

Figure 2. The study design of comparative PK, phase I clinical trial.

The study was approved by the Ministry of Food and Drug Safety of the Republic of Korea and Institutional Review Board of Seoul National University Hospital (Seoul, Republic of Korea). The study was conducted in accordance with the International Conference on Harmonization Good Clinical Practice and the ethical principles of the Declaration of Helsinki. All subjects gave written informed consent prior to enrollment. Demographic data, biochemical indices, and PK sampling information from healthy subjects were included in the database along with plasma concentrations.

2.2. Sample Collection and Analytical Methodology

Blood samples were collected before study drug administration (0 h) and 0.33 h, 0.67 h, 1 h, 1.5 h, 2 h, 2.5 h, 3 h, 4 h, 6 h, 8 h, 10 h, 12 h, 24 h, 34 h, 48 h after study drug administration. Total 16 blood samples were collected from each healthy volunteer. The obtained blood samples (5 mL) were immediately collected into EDTA-K2 tubes and centrifuged for 10 minutes at 3000 rpm and 4° C within 30 minutes. Plasma was aliquoted and stored below -70° C until analysis.

The plasma concentrations of empagliflozin were quantified using a developed and validated liquid chromatography with tandem mass spectrometry (LC-MS/MS) method in accordance with good

laboratory practice standards. The LC-MS/MS system was equipped with a Shimadzu UFLC system (Shimadzu, Kyoto, Japan) and an API5000(3) triple quadrupole mass spectrometer (SCIEX, CA, USA). We used 1 mg/mL empagliflozin-d4 as an internal standard for calibration. The internal standard (10 μL) and methyl tert-butyl ether (1 mL) were added to each 100 μL plasma sample. The ether mix was vortexed for 3 minutes, centrifuged at 13000 rpm for 3 minutes, and stored at -80° C for 20 minutes. The ether layer was transferred to another tube and evaporated under a stream of nitrogen gas. Then, 300 μL of 50% acetonitrile was added and a multi-vortexer was used to solubilize the residue. Five microliters of this solution were injected into the LC-MS/MS system for analysis.

2.3. Base Model Development

The pop-PK analysis was conducted by a nonlinear mixed effect (NLME) modeling approach [21, 22] which was built through estimation by maximum likelihood using the Stochastic Approximation Expectation Maximization (SAEM) algorithm in Monolix® Suite 2021R1 (Lixoft, France) [23].

In previous published studies of pop-PK analysis of empagliflozin in patients, the pop-PK models were developed by two-compartment model with lag time [24-26] and two-

compartment model with transit compartment [19]. Although the biphasic elimination phase was observed in the previous studies which indicated the two-compartment model may be the best to describe PK of empagliflozin [11]. In this study, both the one- and two-compartment models were tested, and all PK processes except absorption were assumed to follow first-order kinetics. The first-order, zero-order, with or without lag time, transit compartment, and Weibull-type absorption models were tested to determine the best description of the absorption profile.

The basic PK model was selected based on the objective function value (OFV) using the log-likelihood ratio test, the value of the Bayesian information criterion (BIC), the goodness-of-fit (GOF) diagnostic plots, and relative standard errors (RSE) of the estimated parameters.

In pop-PK models, unexplained random variability includes IIV, IOV and residual error variability [27]. Because of the crossover study design, the random variation in the pop-PK parameters was described by both IIV and IOV with all individual parameters were considered to be log-normally distributed. IIV and IOV on parameters were sequentially implemented and being then removed or fixed to low values when converging to zero.

The IIV and IOV with an exponential random effects terms

were shown in formula 1 and 2, respectively,

$$P_{ki} = \theta_k \times e^{\eta ki} \quad (1)$$

where P_{ki} represents the parameter value k from the individual i and θ_k describes the population value of the parameter k. ηki denotes the difference between P_{ki} and θ_k.

$$P_{kiq} = \theta_k \times e^{\eta ki + Kkiq} \quad (2)$$

where P_{kiq} is the individual parameter value k from the individual i at the occasion q that differs from the typical individual value by an additional random effect Kkiq. An occasion was characterized as the time period from the start of an infusion and until the start of the next administration. ηki and Kkiq were assumed to be symmetrically distributed with a zero mean and a variance of σ^2 and γ^2, respectively.

Also, we explored the additive, proportional, combined (additive and proportional), and exponential error models to model the residual unexplained variability.

2.4. Covariate Analysis

From the base model (without covariate), the effect of the following 13 covariates on empagliflozin PK parameters was evaluated: treatment, age, height, weight, body mass index (BMI), sex, glucose, protein, aspartate aminotransferase (AST), alkaline phosphatase (ALP), alanine transaminase (ALT), lactate dehydrogenase (LDH)

and estimated glomerular filtration rate (eGFR) levels. The potential covariates were selected according to the plausible mechanism for their influence on PK variability and previous pop-PK of empagliflozin in patients [19].

Data visualization was used to examine the relationship between intrinsic or extrinsic factors and subject-level PK parameters. Initial selection of covariates was guided by graphic inspection and biological plausibility. Potential covariates were tested further in Monolix. Conditional sampling use for stepwise approach based on correlation tests (COSSAC) was used for covariate search. The iterations of COSSAC alternated between a forward selection and a backward elimination, depending on the results of the correlation tests. The final model was derived from the covariates model by excluding covariates that had poor precision where the confidence interval included no effect.

2.5. Internal Evaluation of Final Model

The established empagliflozin population pharmacokinetic model was comprehensively evaluated for GOF plots, visual predictive check (VPCs) (n=500), bootstrapping (n=1000), and normalized prediction distribution error. GOF evaluation was performed by plotting the corresponding individual predictions (IPRED) and population

predictions (PRED) against the observed values as well as the PRED and time against conditional weighted residual errors (CWRES).

A bootstrap resampling was used to assess the reliability and stability of the pop-PK model. A total of 1000 replicates were generated by repeated random sampling with replacement from the original dataset. Estimated parameter values and medians from the bootstrap procedure were compared with those estimated from the original dataset. All processes of model evaluation and validation were performed using R version 4.2.0.

2.6. External Evaluation of Final Model

Empagliflozin and CKD-370 data from an external study were used for the external model evaluation. The external study is a phase I, randomized, crossover clinical study on the comparison PK of 5mg empagliflozin and metformin fixed dose combination (FDC) and 5mg CKD370 and metformin FDC (NCT03848637) [28]. Since metformin and empagliflozin have no common pathway for metabolism or any common transporters, PK interactions are less likely. The data of this external study were thought to be appropriate.

In the external evaluation, model diagnostic plots and the VPCs were generated as for the internal evaluation. Predictive performance of the model was further evaluated by computing bias and precision.

The prediction error (PE) and absolute prediction error (APE) as a measures of bias were calculated according to the IPRED and observed concentrations. Median prediction error (MDPE) and median absolute prediction error (MDAPE) were used to evaluate the accuracy and precision. IF_{20} and IF_{30}, which represented the percentage of individual PE falling within 20% and 30% were also calculated. MDPE% $\leq \pm$ 20%, MDAPE% $\leq$ 30%, $IF_{20} \geq$ 35% and $IF_{30} \geq$ 50% were used to assess the accuracy and precision of the model [29, 30]. Furthermore, mean prediction error (MPE) was calculated within ±20% and ±30% was considered acceptable [31]. The formulas are shown below,

$$\mathrm{PE}(\%) = \frac{P_i - R_i}{R_i} \times 100\% \quad (3)$$

$$\mathrm{APE}(\%) = \left|\frac{P_i - R_i}{R_i}\right| \times 100\% \quad (4)$$

$$\mathrm{MDPE}(\%) = \mathrm{MEDIAN}\left(\frac{P_i - R_i}{R_i} \times 100\%\right) \quad (5)$$

$$\mathrm{MDAPE}(\%) = \mathrm{MEDIAN}\left(\frac{|P_i - R_i|}{R_i} \times 100\%\right) \quad (6)$$

$$\mathrm{MPE}(\%) = \frac{1}{N} \times \sum_{i=1}^{N}\left(\frac{P_i - R_i}{R_i}\right) \times 100\% \quad (7)$$

, where N represents the number of observations, Pi represents the prediction value from the individual i and Ri describes the observation value of the individual i.

Chapter 3. Results

3.1. Demographics and Datasets

The data included 27 healthy subjects (22 males and 5 females) and total 864 plasma concentrations (432 plasma concentrations for each formulation) were included for model building and internal model evaluation. Among them, 2 empagliflozin concentrations and one concentration tested from CKD-370 were below the limit of quantification (BLQ) and marked as uncensored. The characteristics for all included subjects are summarized in Table 1.

Table 1. Demographic and biochemical information of the studied subjects (n = 27).

Physicochemical Parameters	Units	Median [Min−Max]	Mean ± SD
Age	Year	29 [20 – 50]	30 ± 7.38
Height	cm	171.2 [156.3 – 186.3]	170.83 ± 7.01
Weight	kg	72.3 [55.6 – 82.1]	69.62 ± 7.74
BMI	kg/m2	24.2 [19.5 – 26.4]	23.84 ± 2.15
Glucose	mg/dL	87 [79 – 96]	87.33 ± 5.67
Protein	g/dL	6.7 [6.2 – 7.2]	6.67 ± 0.25
ALP	IU/L	52 [30 – 83]	54.44 ± 14.19
AST	IU/L	17 [12 – 27]	17.37 ± 4.1
ALT	IU/L	17 [8 – 47]	18.56 ± 8.93
LDH	IU/L	147 [128 – 219]	155.11 ± 23.04
eGFR	mL/min/1.73m2	115 [74.4 – 143.9]	111.57 ± 15.79

Min, minimum; Max, maximum; BMI, body mass index; ALP, alkaline phosphatase; AST, aspartate aminotransferase; ALT, alanine aminotransferase; LDH, lactate dehydrogenase; eGFR, estimated glomerular filtration rate using MDRD equation.

3.2. Development of Base Model

In this study, one-compartment, two-compartment model with first-order absorption and elimination were tested. One-compartment model showed poor fitness, while two-compartment with lag time and two-compartment with transit compartment model showed similar fit according to the GOF plots. By comparing the OFV and BIC values, a two-compartment transit model was chosen (Table 2). The structural representation of the base model was shown in Figure 3.

Table 2. Comparison of different pharmacokinetic models of empagliflozin.

No.	PK model	OFV	BIC
1	One-compartment with first order (no absorption delay)	8423.73	8467.1
2	One-compartment with first order (with absorption lag time)	8356.88	8410.25
3	Two-compartment with first order (no absorption delay)	8088.96	8152.32
4	Two-compartment with first order (Weibull-type absorption)	7958.11	8021.94
5	Two-compartment with first order (with absorption lag time)	7855.59	7928.95
6*	Two-compartment with first order (add transit compartment)	7811.62	7894.97
7**	Two-compartment with first order (with 6 transit compartments)	7116.59	7217.28

OFV, objective function value; BIC, Bayesian information criterion.

*Selected as final structural model

** Final developed model

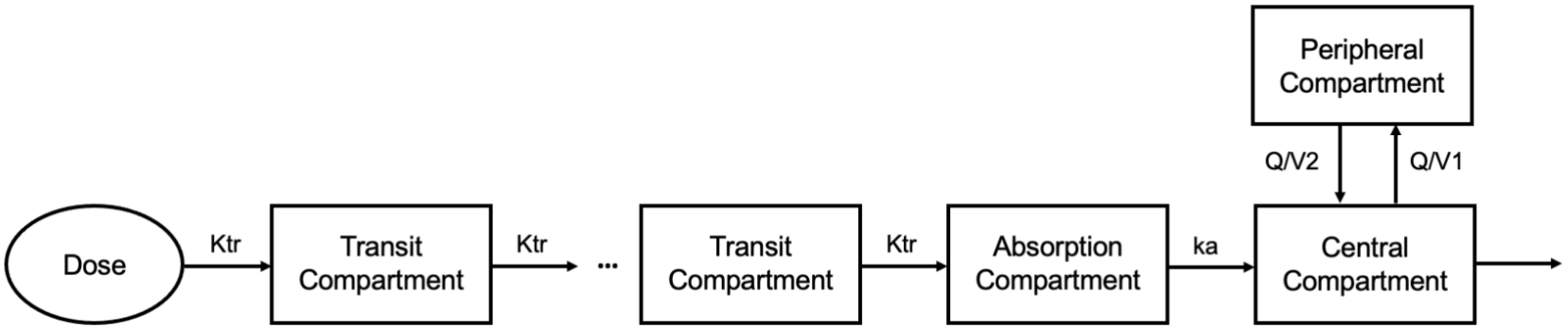

Figure 3. Empagliflozin pop-PK model. 2-compartment transit model with first-order absorption and elimination best fitted observed empagliflozin plasma concentrations.

Ktr, transit rate constant; ka, absorption rate constant; Q, inter-compartmental clearance.

In several test models described in the method, the combined error model was found to best describe the residuals (formula 8),

$$Y_{ij} = C_{ipred,ij} \times (1 + \varepsilon_{prop,ij}) + \varepsilon_{add,ij} \quad (8)$$

where Y_{ij} stands the j^{th} observed concentration in the i^{th} subject and $C_{ipred,ij}$ stands the j^{th} predicted value in the i^{th} subject. Residual error for each observation has therefore a proportional component $\varepsilon_{prop,ij}$ and an additive component $\varepsilon_{add,ij}$, which are normally distributed with mean of 0 and variances σ_{prop}^2 and of σ_{add}^2, respectively.

In conclusion, a 2-compartment with transit compartment model with first-order absorption and elimination, and combined error model were selected as the base model.

3.3. Covariate Analysis

Covariates of interest, which are presented in Table 1 were included in the covariate model development. Covariates were assessed on selected parameters using the COSSAC algorithm. The covariate search results showed that inclusion of treatment on transit rate constant (Ktr), log transformed weight on clearance (CL) and the volume of distribution in peripheral compartment (V2), sex on V2, and ALP on inter-compartmental clearance (Q) significantly improved the model fitting, while ALP was excluded because it was

statistically but not clinically relevant on Q. Additionally sex on V2 was dropped from the final model because of the poor estimation precision (% relative standard error >70).

Finally, IIV on absorption rate constant (Ka), CL, V2, and IOV on Ktr, mean transit time (Mtt), Ka, CL, volume of distribution in central compartment (V1) best described the data. The output of the final model is summarized in Table 3. The small shrinkage of random effect are presented in Table S1. The number of transit compartment was confirmed as six by the formula 9. Most of the PK parameters for the final model were estimated with good precision (i.e., small % RSE), suggesting adequate reliability.

$$\mathrm{Mtt} = \frac{n+1}{K_{tr}} \quad (9)$$

In the comparative PK clinical study, the median values of time to maximum plasma concentration (t_{max}) of two empagliflozin formulations were the same, as 1.5h, however, the minimum t_{max} of empagliflozin and CKD-370 were 0.67h and 1h, respectively.

Slightly slower absorption phase of CKD-370 can be confirmed that the absorption of CKD-370 is approximately 0.54 times that of empagliflozin. The relationship can be presented as the formula shown below

$$\mathrm{K_{tr,i}} = \theta_{\mathrm{ktr,pop}} \times e^{\beta_{\mathrm{ktr,TRT=1}}} \times e^{\eta_{\mathrm{occ,ktr}}} \quad (10)$$

,where θ represents the fixed-effect parameters. i means the predicted value of i^{th} patient. TRT was category covariate where TRT= 0 indicates empagliflozin, TRT= 1 indicates CKD-370.

Table 3. Estimates of the population pharmacokinetics parameter.

Population Parameter (Unit)	Value	RSE (%)	Median of Bootstrap* (95% CI)
Fixed effects			
Ktr (h^{-1})	10.96	18.0	10.66 (6.958 – 22.339)
Mtt (h)	0.63	7.29	0.63 (0.53 – 0.743)
Ka (h^{-1})	0.28	5.64	0.28 (0.229 – 0.375)
CL (L/h)	8.17	2.38	8.13 (7.474 – 8.482)
V1 (L)	1.53	35.0	1.54 (0.312 – 3.186)
V2 (L)	43.67	2.95	43.68 (39.369 – 61.846)
Q (L/h)	5.82	7.27	5.51 (4.011 – 8.534)
β Ktr_Treatment[a]	− 0.61	39.3	−0.53 (−1.071 – −0.069)
β CL_logWT	1.01	21.0	1.03 (0.672 – 1.883)
β V2_logWT	0.86	23.7	0.82 (−3.585 – 1.293)
Inter−individual variability (IIV)[b]			
ω Ka (%)	0.21 (21.23)	15.5	0.21 (0.126 – 0.719)

ωCL (%)	0.12 (12.04)	16.0	0.11 (0.081 – 0.214)
ωV2 (%)	0.098 (9.82)	19.6	0.1 (0.066 – 0.931)
Inter-occasion Variability (IOV)[b]			
γKtr (%)	0.75 (86.89)	15.5	0.76 (0.541 – 1.335)
γMtt (%)	0.42 (43.92)	12.5	0.43 (0.29 – 0.589)
γKa (%)	0.055 (5.50)	42.0	0.07 (0.034 – 0.115)
γCL (%)	0.05 (5.00)	21.0	0.05 (0.019 – 0.076)
γV1 (%)	1.36 (231.46)	19.0	1.43 (0.994 – 2.566)
Residual variability			
a	0.58	21.4	0.64 (0.014 – 1.059)
b	0.12	4.26	0.12 (0.105 – 0.152)

* from 1000 bootstrap resampling.

a: Treatment of CKD-370.

b: IIV and IOV are presented as SD (CV).

RSE, relative standard errors; CI, confidence interval; Ktr, identical transfer rate constant of the transit compartment model; Mtt, mean transit time for the absorption; SD, standard deviation; CV: coefficient of variation.

3.4. Internal Evaluation of Final Model

The performance of the final model was evaluated by both internal and external validations. Figure 4 shows results of GOF plots for the final pop-PK model of empagliflozin. Figures 4A, B showed that there was no systematic bias on predictions. As shown in Figures 4C, D, no trends were found in the diagnostic plots of population weighted residuals (PWRES) versus time and population prediction (PRED). The NPDE results were shown in Figures 5. As shown in Figures 5A, B, NPDE distribution and histogram agreed well with the standard normal distribution and density, which indicates that the model fitted to the individual data well. As shown in Figures 5C, D, there was no trend in NPDE versus time and PRED. The results of the VPC with 500 simulations for the final pop-PK model proved the appropriateness of the final model (Figure 6).

Table 3 shows bootstrapping and RSE results for the final pop-PK model established for empagliflozin. The RSE values were small, and all the parameter values estimated with this final model were within 95% confidence intervals(CIs) of bootstrap analysis results (number of replication: 1000). Estimated values of model parameters were almost similar to the median estimated by bootstrap analysis. Results of bootstrapping analysis confirmed the robustness and reproducibility of the final pop-PK model established for

empagliflozin. The final model with covariates is considered as representative. Overall, the estimated IIV and IOV adequately described the observed variability in empagliflozin concentrations. Empagliflozin concentrations were well characterized by the final pop-PK model.

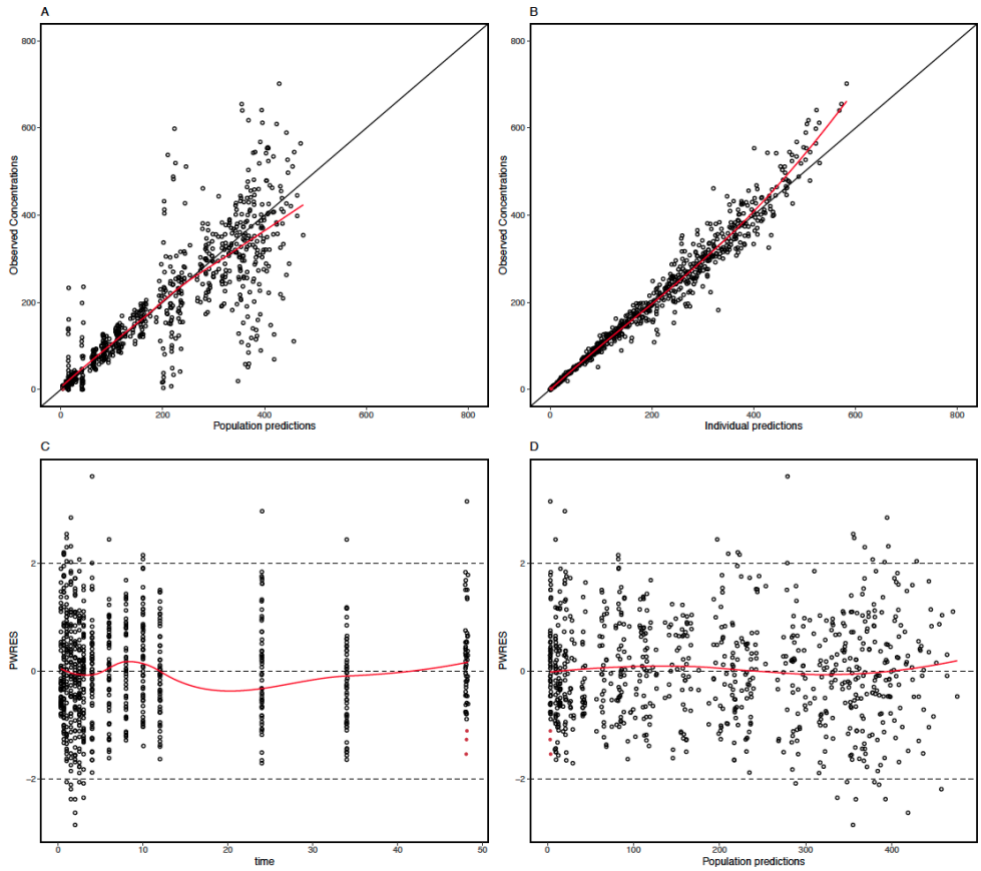

Figure 4. Goodness-of-fit plots of final population pharmacokinetic model for empagliflozin. (A) Population predicted concentrations (PRED) against observed plasma concentration; (B) Individual-predicted concentrations (IPRED) against observed plasma concentration; (C) Time against conditional weighted residuals; (D) PRED against conditional weighted residuals. Red dots mean the data are not censored.

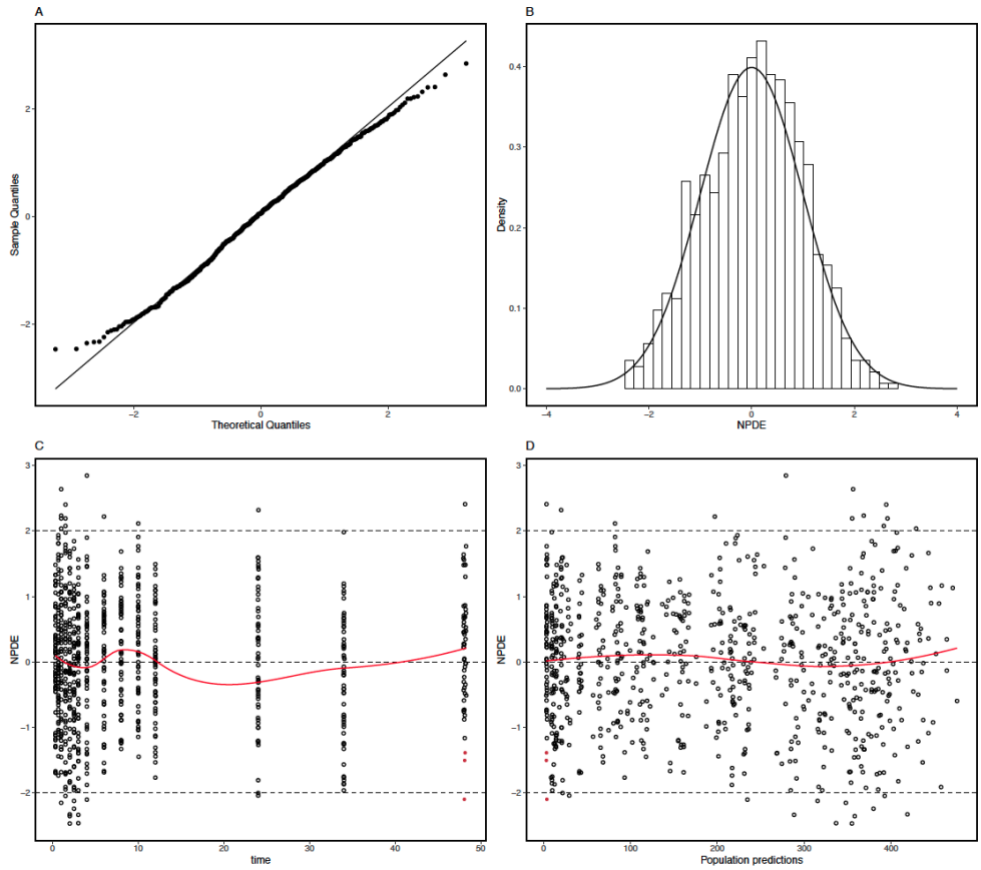

Figure 5. Normalized prediction distribution error (NPDE) metrics for the population pharmacokinetic model of cefepime. Normal Q–Q plot for NPDE (A), distribution of NPDE (B), and NPDE versus time after first dose (C) and versus predicted concentrations (D).

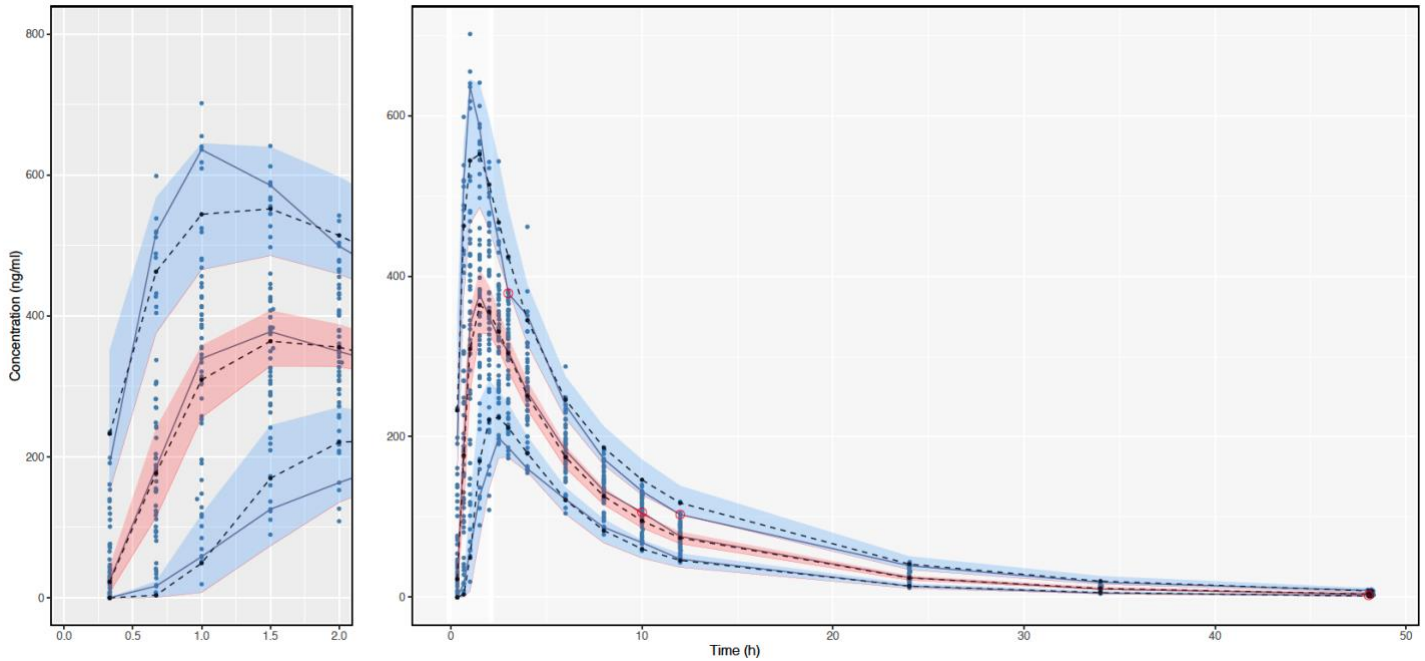

Figure 6. Visual predictive check (500 simulations) of the final model for empagliflozin. Observed concentrations were depicted by dots. Blue solid lines indicate 95th, 50th, and 5th percentiles of predicted concentrations. Black dash lines indicate the predicted mean. Blue shaded regions indicate 95% confidence intervals for predicted 5th and 95th percentiles. Pink shaded regions indicate 95% confidence intervals for the predicted 50th percentiles. Outliers are highlighted with red dots and areas.

3.5. External Evaluation of Final Model

The external data were obtained from another clinical study (NCT03848637) which included 27 healthy subjects (20 males and 7 females) and total 968 plasma concentrations (485 plasma concentrations for empagliflozin and 483 plasma concentrations for CKD-370). Three empagliflozin concentrations and three CKD-370 concentration were BLQ and marked as uncensored. Characteristics for subjects from external dataset were summarized in Table 4. External evaluation confirmed that the model can predict the drug concentration of single oral dose of 5 mg empagliflozin and CKD-370 prospectively by diagnostic plots (Figure 7), NPDE plots (Figure 8) and VPCs (Figure 9). The IF_{20} and IF_{30} were calculated as 36.88% and 53.1%, respectively. MDPE was calculated as -0.4%, MDAPE was calculated as 24.4% and MPE was calculated as 22.01%, which suggested that the final model showed accurate precise predictions.

Table 4. Demographic and biochemical information of the subjects in the external evaluation dataset (n = 27).

Physicochemical Parameters	Units	Median [Min–Max]	Mean ± SD
Age	Year	27 [21 – 47]	30.22 ± 7.71
Height	cm	172.4 [155.2– 186.4]	171.60 ± 7.64
Weight	kg	70.1 [56.1 – 83.4]	69.76 ± 8.05
BMI	kg/m2	23.9 [19.8 – 26.9]	23.65 ± 1.95
Glucose	mg/dL	87 [78 – 101]	88.07 ± 6.34
Protein	g/dL	6.7 [6.3 – 7.4]	6.71 ± 0.26
ALP	IU/L	59 [36 – 81]	58.63 ± 11.98
AST	IU/L	17 [13 – 35]	17.85 ± 4.88
ALT	IU/L	16 [7 – 64]	19.44 ± 12.20
LDH	IU/L	147 [113 – 185]	145 ± 19.80
eGFR	mL/min/1.73m^2	111.9 [74.2 – 138.7]	110.77 ± 15.74

Min, minimum; Max, maximum; BMI, body mass index; ALP, alkaline phosphatase; AST, aspartate aminotransferase; ALT, alanine aminotransferase; LDH, lactate dehydrogenase; eGFR, estimated glomerular filtration rate using MDRD equation.

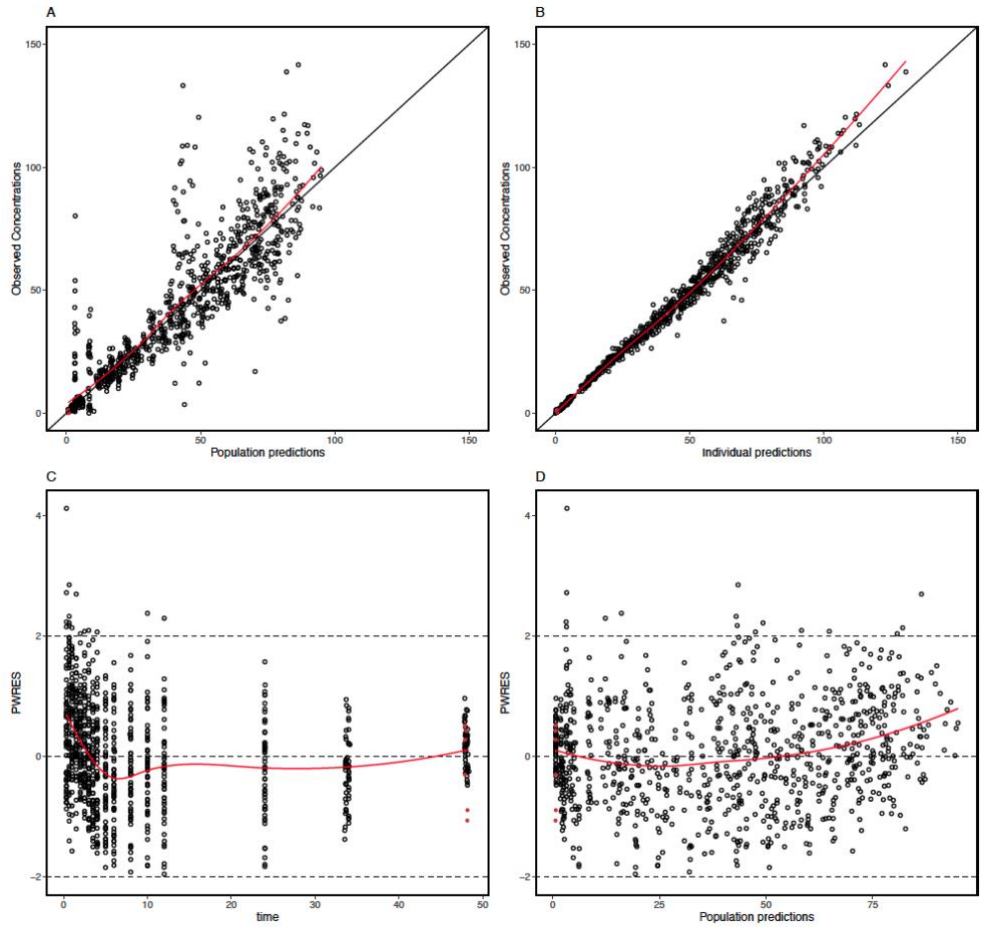

Figure 7. Goodness-of-fit plots for external model evaluation. (A) Population-predicted concentrations (PRED) against observed plasma concentration; (B) Individual-predicted concentrations (IPRED) against observed plasma concentration; (C) Time against conditional weighted residuals; (D) PRED against conditional weighted residuals. Red dots mean the data are not censored.

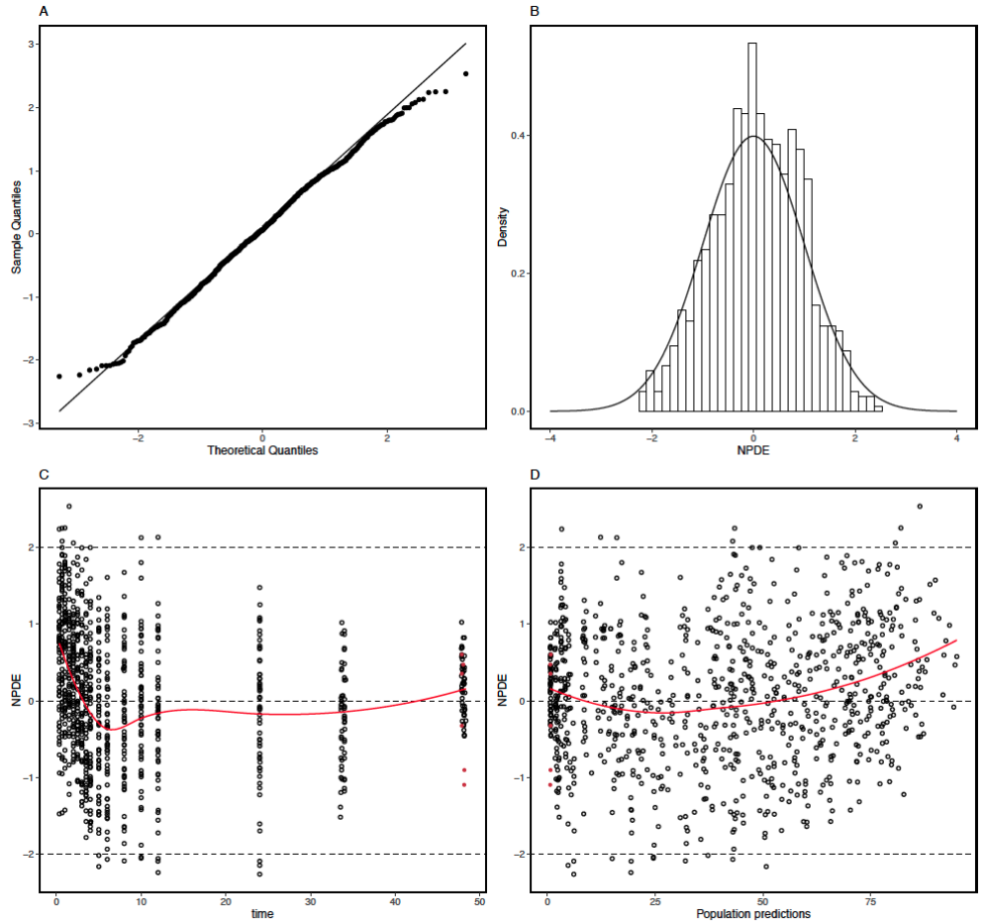

Figure 8. NPDE for the validation set. a Q−Q plot. b Histogram of NPDE. Theoretical distribution represented as shaded bars. c NPDE versus time after dose (TAD). Prediction intervals represented as shaded areas. Observations plotted as circles and observation percentiles as solid lines. d NPDE versus PRED.

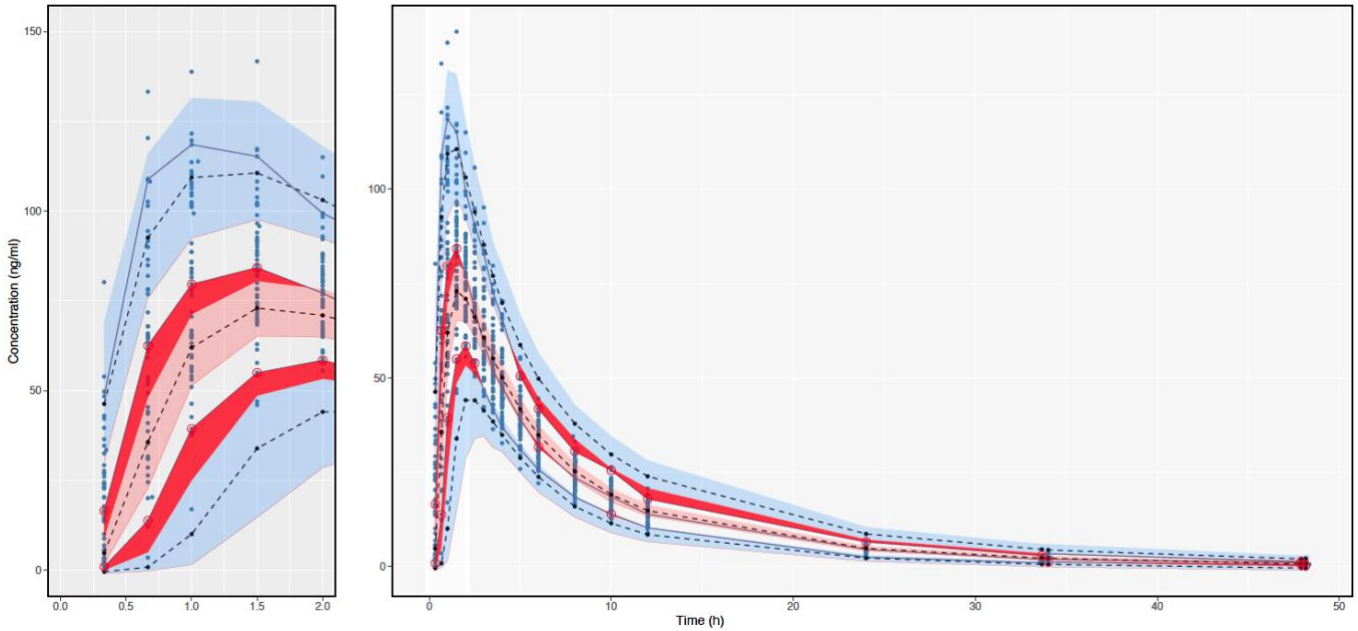

Figure 9. Visual predictive check (500 simulations) of the external model evaluation. Observed concentrations were depicted by dots. Blue solid lines indicate 95th, 50th, and 5th percentiles of predicted concentrations. Black dash lines indicate the predicted mean. Blue shaded regions indicate 95% confidence intervals for predicted 5th and 95th percentiles. Pink shaded regions indicate 95% confidence intervals for the predicted 50th percentiles. Outliers are highlighted with red dots and areas.

Chapter 4. Discussion

Cocrystal technology is famous as changing drugs' chemical properties and improving drug's oral absorption [17]. In the previous studies, the bioequivalence of these two formulations were verified, the bioavailability of these two formulations seem the same. The primary PK parameters and PK profile were shown in the Table 5 and Figure 10 showing a small difference in the absorption of the two formulations. Thus, in this study, we investigated the differences of absorption phase by using pop-PK analysis. So far, there were 3 pop-PK analysis studies of empagliflozin, which were all conducted in patients. Herein, we reported the first pop-PK analysis for two different empagliflozin formulations in healthy subjects and explored various absorption models.

The previous study, except two-compartment with lagged first-order oral absorption with lag time fixed as 0.5 hours could appropriately describe empagliflozin plasma concentration data [25], also three transit compartments with an estimated Mtt, which means the average time spent by drug molecules traveling from the first transit compartment to the absorption compartment of approximately 30 minutes were included in series to precede a first-order absorption compartment [19]. In our study, PK of empagliflozin was

modeled as two-compartment model with six transit compartments with first order absorption and elimination, and the Mtt was 37.8 minutes, which was similar to the value in the previous study.

Individual parameters can vary from individuals and occasions, thus both IIV and IOV need to be studied if data was collected in different occasions when developing pop-PK model [32]. Although IOV has long been recognized to be of importance in non-linear mixed effect [33], all of the pop-PK studies on empagliflozin didn't include the IOV part. In this study, various errors (including residual error, IIV and IOV) models and covariate effects were evaluated to establish factors that significantly influence the PK parameters of empagliflozin and to explain the PK diversity of the empagliflozin in the population. The results suggested that the log-transformed weight and the treatment were the covariate of IIV on CL, V2, and IOV on treatment, respectively. The shrinkage values based on SD were all smaller than 30% (Table 6), indicating the model was credible for covariate exploration.

Table 5. Summary of pharmacokinetic parameters of two empagliflozin formulations in plasma after single oral dose.

Pharmacokinetic parameters	5mg CKD-370 (N=27)	5mg Empagliflozin (N=27)	25mg CKD-370 (N=27)	25mg Empagliflozin (N=27)
T_{max} (h)	1.50 [1.00 – 2.50]	1.50 [0.67 – 2.50]	1.50 [1.00 – 4.00]	1.50 [0.67 – 4.00]
C_{max} (μg/L)	94.21 ± 16.69	91.84 ± 18.72	442.02 ± 103.37	436.29 ± 118.74
AUC_{last} (μg · h/L)	614.59 ± 90.77	598.81 ± 90.24	3131.08 ± 529.30	3006.88 ± 514.21
AUC_{inf} (μg · h/L)	631.43 ± 86.39	611.94 ± 91.40	3194.53 ± 547.43	3064.17 ± 522.99
$t_{1/2}$ (h)	8.89 ± 1.78	9.01 ± 1.88	8.62 ± 1.45	8.59 ± 1.52
CL/F (L/h)	8.07 ± 1.14	8.35 ± 1.24	8.06 ± 1.46	8.41 ± 1.54
V_d/F (L)	103.20 ± 24.77	108.13 ± 26.88	99.82 ± 22.51	103.49 ± 22.49

Data are presented as arithmetic mean ± standard deviation, except for T_{max} presented as median [minimum-maximum].

T_{max}, time to maximum plasma concentration; C_{max}, maximum plasma concentration; AUC_{last}, area under the plasma drug concentration-time curve from 0 to last; AUC_{inf}, area under the plasma drug concentration-time curve from 0 to infinity; $t_{1/2}$, half-life; CL/F, apparent clearance; V_d/F, apparent volume of distribution.

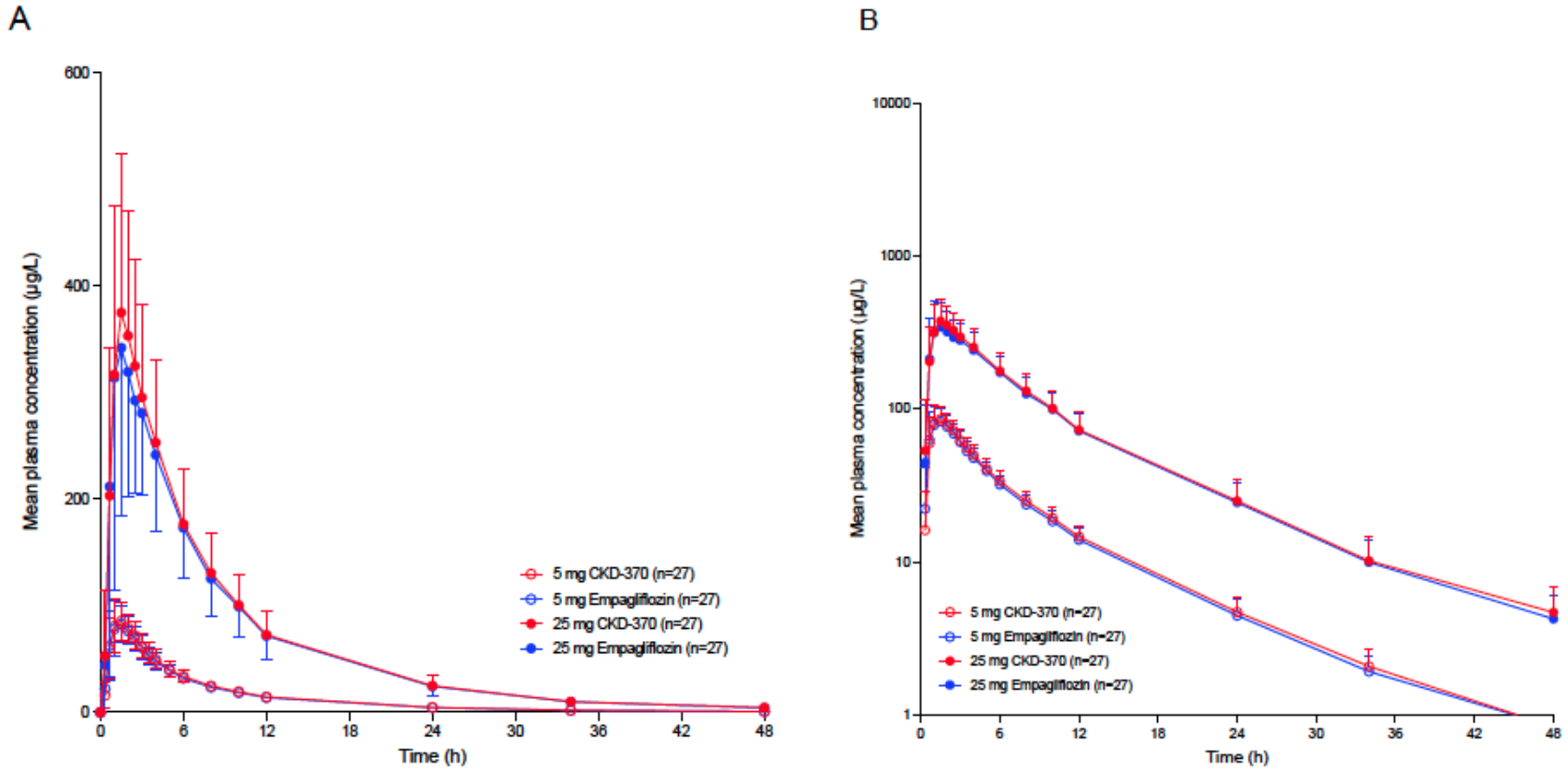

Figure 10. Mean (SD) plasma concentration-time profile for single dose administration of two empagliflozin formulations in (A) linear scale and (B) log scale.

Table 6. Shrinkage of PK parameters.

PK parameter (Unit)	Based on variance [a]	Based on SD [b]
Ktr (h^{-1})	28.5%	15.44%
Mtt (h)	24.7%	13.22%
Ka (h^{-1})	7.1%	3.62%
CL (L/h)	6.32%	3.21%
V1 (L)	41.9%	23.78%
V2 (L)	30.6%	16.69%

a: Shrinkage was calculated by the formula with variance which is often used in Monolix

$$\eta\text{-}sh = 1 - \frac{var(\eta_i)}{\omega^2}$$

b: Shrinkage was calculated by the formula with standard deviation which is often used in NONMEM

$$\eta\text{-}sh = 1 - \frac{sd(\eta_i)}{\omega}$$

It is notable that unlike most studies in this study we also performed an external evaluation of the model with a new set of data to support the prediction of the final empagliflozin PK model. Concentration data of 25 mg of both formulations were used for the model development and internal evaluation, while 5 mg of both formulations were used for the model external evaluation, indicating that the model accurately predicted the dosing regimen at different

dosage strengths. The GOF plots and VPCs showed slightly underestimation in the absorption phase (Figure 7, 9), which may be due to differences in dose-strength. Additionally, CKD-370 showed the slower absorption than empagliflozin, which may be because the co-crystallization form that CKD-370 broken down to empagliflozin in the digestive system needs time. The slower absorption was not considered clinically meaningful as the two formulations had previously been demonstrated to be bioequivalent. In this study, the log-transformed weight was used as covariate, which means that the dosing regimen study in children who have low body weight can be studied in the future.

Furthermore, the study had some limitations. It is noteworthy that the PK profiles of a single dose of 25 mg empagliflozin tablet in previous studies have been reported in healthy Caucasian, Egyptian, Japanese, and Chinese subjects [7-10]. The study in South Korea provided further information about the impact of different human race on the PK parameters of empagliflozin. Comparing the main PK parameters with those data obtained from previous studies, we found that the C_{max} and AUC_{last} for both two formulations were similar to that in Chinese and Japanese subjects, but higher than that in Egyptian and Caucasian subjects. Therefore, the developed pop-PK model may be not fit in healthy subjects with other races.

Chapter 5. Conclusion

The pop-PK model for empagliflozin was well described by a 2-compartment model with 6 transit compartments with first-order absorption and elimination in healthy Korean volunteers. A slightly slower absorption phase of CKD-370 can be confirmed that the absorption of CKD-370 is approximately 0.54 times that of empagliflozin, which indicates that CKD-370 broken down to empagliflozin in the digestive system needs time. Because the bioequivalence was proved in the previous study, the absorption difference between the two formulations is not clinically meaningful.

Bibliography

1. Green, A., et al., *Type 1 diabetes in 2017: global estimates of incident and prevalent cases in children and adults.* Diabetologia, 2021. **64**(12): p. 2741-2750.
2. Salinas, L.F., et al., *Impaired rate-dependent depression of the H-reflex in type-2 diabetes, prediabetes, overweight and obesity: A cross-sectional study.* Medicine (Baltimore), 2022. **101**(43): p. e31046.
3. Zheng, Y., S.H. Ley, and F.B. Hu, *Global aetiology and epidemiology of type 2 diabetes mellitus and its complications.* Nat Rev Endocrinol, 2018. **14**(2): p. 88-98.
4. Rieg, T. and V. Vallon, *Development of SGLT1 and SGLT2 inhibitors.* Diabetologia, 2018. **61**(10): p. 2079-2086.
5. Kavanagh, O.N., et al., *Pharmaceutical cocrystals: from serendipity to design to application.* Drug Discov Today, 2019. **24**(3): p. 796-804.
6. Tamura, H., et al., *Comparison of the effects of empagliflozin and glimepiride on endothelial function in patients with type 2 diabetes: A randomized controlled study.* PLoS One, 2022. **17**(2): p. e0262831.
7. Li, X., et al., *Pharmacokinetics and bioequivalence of a generic*

empagliflozin tablet versus a brand-named product and the food effects in healthy Chinese subjects. Drug Dev Ind Pharm, 2020. **46**(9): p. 1487-1494.

8. Ayoub, B.M., et al., *Pharmacokinetic Evaluation of Empagliflozin in Healthy Egyptian Volunteers Using LC-MS/MS and Comparison with Other Ethnic Populations.* Sci Rep, 2017. **7**(1): p. 2583.

9. Sarashina, A., et al., *Safety, tolerability, pharmacokinetics and pharmacodynamics of single doses of empagliflozin, a sodium glucose cotransporter 2 (SGLT2) inhibitor, in healthy Japanese subjects.* Drug Metab Pharmacokinet, 2013. **28**(3): p. 213-9.

10. Seman, L., et al., *Empagliflozin (BI 10773), a Potent and Selective SGLT2 Inhibitor, Induces Dose-Dependent Glucosuria in Healthy Subjects.* Clin Pharmacol Drug Dev, 2013. **2**(2): p. 152-61.

11. Scheen, A.J., *Pharmacokinetic and pharmacodynamic profile of empagliflozin, a sodium glucose co-transporter 2 inhibitor.* Clin Pharmacokinet, 2014. **53**(3): p. 213-225.

12. Yadav, A.V., et al., *Co-crystals: a novel approach to modify physicochemical properties of active pharmaceutical ingredients.* Indian J Pharm Sci, 2009. **71**(4): p. 359-70.

13. Gadade, D.D. and S.S. Pekamwar, *Pharmaceutical Cocrystals: Regulatory and Strategic Aspects, Design and Development.* Adv Pharm Bull, 2016. **6**(4): p. 479-494.

14. Shan, N., et al., *Impact of pharmaceutical cocrystals: the effects on drug pharmacokinetics.* Expert Opin Drug Metab Toxicol, 2014. **10**(9): p. 1255-71.

15. Guo, M., et al., *Pharmaceutical cocrystals: A review of preparations, physicochemical properties and applications.* Acta Pharm Sin B, 2021. **11**(8): p. 2537-2564.

16. Cho, H.J., et al., *Novel dapagliflozin di-L-proline cocrystal-loaded tablet: preparation, physicochemical characterization, and pharmacokinetics in beagle dogs and mini-pigs.* Pharm Dev Technol, 2022. **27**(3): p. 331-340.

17. Emami, S., et al., *Recent advances in improving oral drug bioavailability by cocrystals.* Bioimpacts, 2018. **8**(4): p. 305-320.

18. Cui, W., et al., *Naringenin Cocrystals Prepared by Solution Crystallization Method for Improving Bioavailability and Anti-hyperlipidemia Effects.* AAPS PharmSciTech, 2019. **20**(3): p. 115.

19. Riggs, M.M., et al., *Population pharmacokinetics of empagliflozin, a sodium glucose cotransporter 2 inhibitor, in*

patients with type 2 diabetes. J Clin Pharmacol, 2013. **53**(10): p. 1028-38.

20. Jiang, X., et al., *Comparison of the Pharmacokinetics, Safety, and Tolerability of Two Empagliflozin Formulations in Healthy Korean Subjects.* Drug Des Devel Ther, 2023. **17**: p. 2137-2145.

21. Lindstrom, M.L. and D.M. Bates, *Nonlinear mixed effects models for repeated measures data.* Biometrics, 1990. **46**(3): p. 673-87.

22. Sheiner, L.B. and T.M. Ludden, *Population pharmacokinetics/dynamics.* Annu Rev Pharmacol Toxicol, 1992. **32**: p. 185-209.

23. Savic, R.M., F. Mentre, and M. Lavielle, *Implementation and evaluation of the SAEM algorithm for longitudinal ordered categorical data with an illustration in pharmacokinetics-pharmacodynamics.* AAPS J, 2011. **13**(1): p. 44-53.

24. Mondick, J., et al., *Population Pharmacokinetic-Pharmacodynamic Analysis to Characterize the Effect of Empagliflozin on Renal Glucose Threshold in Patients With Type 1 Diabetes Mellitus.* J Clin Pharmacol, 2018. **58**(5): p. 640-649.

25. Baron, K.T., et al., *Population Pharmacokinetics and*

Exposure-Response (Efficacy and Safety/Tolerability) of Empagliflozin in Patients with Type 2 Diabetes. Diabetes Ther, 2016. **7**(3): p. 455-71.

26. Riggs, M.M., et al., *Exposure-response modelling for empagliflozin, a sodium glucose cotransporter 2 (SGLT2) inhibitor, in patients with type 2 diabetes.* Br J Clin Pharmacol, 2014. **78**(6): p. 1407-18.

27. Abrantes, J.A., et al., *Handling interoccasion variability in model-based dose individualization using therapeutic drug monitoring data.* Br J Clin Pharmacol, 2019. **85**(6): p. 1326-1336.

28. Lee, H., et al., *Pharmacokinetic Comparison Between a Fixed-Dose Combination of Empagliflozin L-Proline/Metformin and Empagliflozin/Metformin in Healthy Korean Subjects.* Clin Pharmacol Drug Dev, 2023.

29. Hara, M., et al., *Predictive performance of eleven pharmacokinetic models for propofol infusion in children for long-duration anaesthesia.* Br J Anaesth, 2017. **118**(3): p. 415-423.

30. Zhao, C.Y., et al., *External evaluation of published population pharmacokinetic models of tacrolimus in adult renal transplant recipients.* Br J Clin Pharmacol, 2016. **81**(5): p. 891-907.

31. Chen, Y., et al., *Population pharmacokinetics of vancomycin and AUC-guided dosing in Chinese neonates and young infants.* Eur J Clin Pharmacol, 2018. **74**(7): p. 921-930.

32. Administration, U.S.D.o.H.a.H.S.F.a.D., *Population Pharmacokinetics Guidance for Industry.* February 2022.

33. Kristoffersson, A.N., L.E. Friberg, and J. Nyberg, *Inter occasion variability in individual optimal design.* J Pharmacokinet Pharmacodyn, 2015. **42**(6): p. 735-50.

Abstract in Korean

서론: 엠파글리플로진은 제2형 당뇨병(T2DM)의 치료에 널리 사용되는 나트륨-포도당 공동수송체 2(SGLT2) 억제제이다. CKD-370은 용매화물 L-프롤린과 엠파글리플로진의 공결정제의 형태로 개발된 신약이며, 국내에서 엠파글리플로진과 CKD-370의 생동성이 확인되었다. 본 연구에서는 건강한 성인을 대상으로 엠파글리플로진 두 제형에 대한 집단약동학(pop-PK) 모델을 개발하고, 두 제형 간의 상관관계를 탐색하며, 다양한 공변량이 엠파글리플로진의 약동학에 어떠한 영향을 미치는지를 조사하였다.

방법: 생동성을 확인하기 위해 수행된 연구에서 총 27명의 건강한 성인으로부터 25mg의 엠파글리플로진의 총 864개 혈장 농도 데이터를 얻었고, 이를 엠파글리플로진의 집단 약동학 분석에 사용하였다. 집단 약동학 모델은 비선형 혼합 효과 접근법을 사용하기 위하여 Monolix Suite 2021R1을 통해서 수행되었다. 데이터셋에 총 13개의 잠재적 공변량이 포함되었다. 개인간변이(IIV)과 기간변이(IOV)을 모두 확인하였다. 최종 모델은 적합도(GOF) 진단 플롯, 시각적 예측 검사(VPC), 예측 오차 및 부트스트래핑을 통해 내부검증 및 외부검증이 수행되었다.

결과: 건강한 성인에서 엠파글리플로진의 약동학은 1차 흡수 및 제거가 있는 2구획 모델과 6개 transit compartment로 적절하게 설명되었다. Log 변환한 체중은 엠파글리플로진의 전신 청소율 및 peripheral compartment의 분포용적에 유의한 영향을 미치는 것을 확인할 수 있다.

CKD-370은 엠파글리플로진보다 더 느린 흡수를 보였다. 최종 모델의 GOF 플롯, VPCs, 예측 오차 및 부트스트래핑을 통해서 최종 모델이 적합성 및 정밀도가 좋은 것을 확인하였으며, 다른 용량에서도 좋은 정확도를 가지고 있음을 확인하였다.

결론: 2개의 엠파글리플로진 제형에 대한 최종 집단 약동학 모델은 건강한 성인에서 관찰된 엠파글리플로진의 혈장 농도를 잘 설명하였다. 이 모델은 두 제형 간의 상관관계와 그들의 약동학적 특성을 이해하는 데 도움이 될 것으로 예상된다. 또한, 건강한 한국인을 대상으로 엠파글리플로진의 집단약동학 모델을 처음으로 구축하였으며, 이는 향후 환자에서 추가 공변량을 탐색하는 데 유용하게 활용할 수 있을 것이다.

주요어: 엠파글리플로진, 엠파글리플로진 L-프롤린(CKD-370), 집단약동학 모델링

학번: 2021-29727